Colloid Polym Sci (1995) 273:165–174

ORIGINAL CONTRIBUTION

V. Bergeron
C. J. Radke

Disjoining pressure and stratification in asymmetric thin-liquid films

Received: 9 April 1994
Accepted: 1 June 1994

Prof. Dr. C. J. Radke (✉)
Currently at Ecole Normale Supérieure
Laboratoire de Physique Statistique
24 Rue Lhomond, 75231 Paris
France, Cedex 05

V. Bergeron
Department of Chemical Engineering
University of California, Berkeley
101 Gilman Hall
Berkeley, California 94720, USA

Abstract We directly measure, for the first time, disjoining pressure isotherms for asymmetric oil/aqueous surfactant/gas (i.e., pseudoemulsion) films using a modified version of the porous-plate technique first developed by Mysels in conjunction with thin-film interferometry. Dynamic film-thinning experiments are also performed on individual foam and pseudoemulsion films. At SDS surfactant concentrations above the critical micelle concentration (CMC) (0.1 M SDS), the pesudoemulsion films exhibit the same step-wise layer thinning observed in foam films under similar conditions. Further, we conduct dynamic thinning experiments on solid/liquid/gas systems and show that aqueous 0.2 M CTAB films sandwiched between glass and air also display discrete thinning transitions. All of these stratification transitions arise from oscillations in the disjoining pressure isotherm, generated by amphiphilic structuring within the film.

For 0.1 M SDS dedecane/air pesudoemuslion films, the slope and peak height of the disjoining-pressure oscillations increase with each subsequent amphiphilic layer as film thickness decreases. Magnitudes of the structural forces are low (< 100 Pa) but the length scale of the oscillations is large (~ 10 nm) and rather far reaching (~ 50 nm). Moreover, for 0.1 M SDS solutions, the capillary pressures associated with film rupture are significantly lower for pseudoemulsion films (~ 0.1 kPa) when compared to foam films (~ 15 kPa) at equivalent conditions. Taken together, our dynamic thinning and equilibrium disjoining pressure measurements indicate that stratification in 0.1 M SDS films has little effect on both kinetic and thermodynamic films stability.

Key words Disjoining pressure – stratification – foam – pseudemulsion – supramolecular structuring

Introduction

Thin-liquid film stability is an important physical phenomenon in surface and colloid science as it arises from fundamental intermolecular interactions within confined geometries. Furthermore, because liquid films are present in many different processes, their stability characteristics are also important from a practical point of view. For example, ore floatation and oil recovery operations depend on control and manipulation of all the thin films present. This includes both symmetric (e.g. foam and emulsion, including oil-in-water and water-in-oil) and asymmetric (e.g., gas/water/oil and gas/liquid/solid) films.

The fundamental property that gauges the thermodynamic stability of thin-liquid films is the disjoining pressure, $\Pi(h)$, which measures the interaction force (per unit area) between two macroscopic bodies as they approach one another. Π is a function of the intervening film thickness, h, and can be either positive (disjoining) or negative (conjoining). Highly positive disjoining pressures imply strong repulsive forces between the bodies and a stable film, whereas negative attractive forces produce unstable films.

Previously, the vast majority of work on thin-liquid films, both experimental and theoretical, has focused only on symmetric films. The framework for these studies originates from the research performed in the middle of this century by Derjaguin [1] and Scheludko [2]. Their achievements are encompassed in the well-known DLVO theory. DLVO theory describes the forces that act between two bodies as resulting from electrostatic repulsive forces that tend to stabilize the intervening film, and London–van der Waals dispersion forces which are typically attractive and destabilize films. This theory has been successful in the past for simple systems, but it does not account for any structural forces that may arise within the film. More specifically, it fails to incorporate forces arising from self-assembling structures that can occur in systems containing surfactant above the critical micelle concentration (CMC).

Recently, Bergeron and Radke [3] experimentally quantified an equilibrium structural component to the disjoining pressure for foam films containing sodium dodecyl sulfate, SDS, at concentrations well above the CMC. They showed that the form of the disjoining pressure isotherm in these systems can be rather complex, revealing an oscillatory component that extends to film thicknesses larger than 50 nm. Similar data have also been recently reported by Richetti and Kékicheff (4) for aqueous micellar films of cetyltrimethylammonium bromide, CTAB, formed between CTAB-coated mica surfaces in a Surface Force Apparatus, SFA. Disjoining pressures in the SFA measurements are significantly higher than those in foam films, but, the same qualitative observations are reproduced. This suggests that the oscillatory component originates from the same physical processes and that the behavior is somewhat universal. It remains to be seen whether or not oscillatory forces are produced in asymmetric systems and what the magnitude of these forces might be.

Of particular interest are asymmetric aqueous films formed between a gas and an oil phase. Such three-phase (oil/water/gas) surfactant-laden films are called pseudoemulsion films [5] and are critical in enhanced oil recovery operations that use foam as an injection fluid [6, 7]. For example, there is considerable evidence that the stability of bulk and porous-media foam in contact with oil is controlled by the thermodynamic stability of pseudoemuslion films [6, 7, 8]. Conversely, there is speculation that supramolecular structuring, generated during the dynamics of film thinning, and referred to as film stratification, contributes to the stability of pseudoemuslion films [5, 9]. Measurements of disjoining pressures are needed to quantify the forces generated in stratifying films. Bergeron and Radke [10] have confirmed stratification in pseudoemulsion films containing surfactant above the CMC, but, disjoining forces were not measured in that study.

Our objective is to quantify any long-range oscillatory forces in asymmetric thin-liquid films at surfactant concentrations above the CMC. We measure directly the disjoining pressure iostherm for dodecane/air pseudoemulsion films made from aqueous solutions of SDS. Disjoining-pressure measurements, together with film-thinning experiments on the same systems determine the importance of supramolecular structuring on both equilibrium and dynamic film stability. Experimental conditions are carefully selected so that a direct comparison between foam and pseudoemulsion films can be made. Finally, we conduct film-thinning experiments on asymmetric gas/aqueous/solid films and demonstrate that these films also display stratification akin to that observed in foam and pseudoemulsion films.

Experimental

Apparatus

The experimental cell used to investigate pseudoemulsion films utilizes the porous-plate technique, originally developed by Mysels [11] and more recently refined by Exerowa et al. [12] for measuring disjoining pressures in aqueous foam films. Single, isolated thin-liquid films are formed in a specially designed hole, bored through a sintered glass disk that has been fused to a 4-mm I.D. capillary tube. This holder is placed in a 200-cm^3 hermetically sealed Plexiglas cell, as shown in Fig. 1. Liquids in the cell are configured such that the less dense oil phase floats on top of the aqueous surfactant solution that is under investigation. This ensures equilibrium between the oil and solution phase during the course of the experiment. A syringe port at the bottom of the cell is used to regulate the amount of solution in the cell, thereby changing the horizontal level of the oil-gas interface. Once the oil level is raised to the base of the porous-glass frit, which has been presaturated with surfactant solution, a pseudoemulsion film can be formed by dropwise addition of aqueous surfactant solution through a syringe port located above the

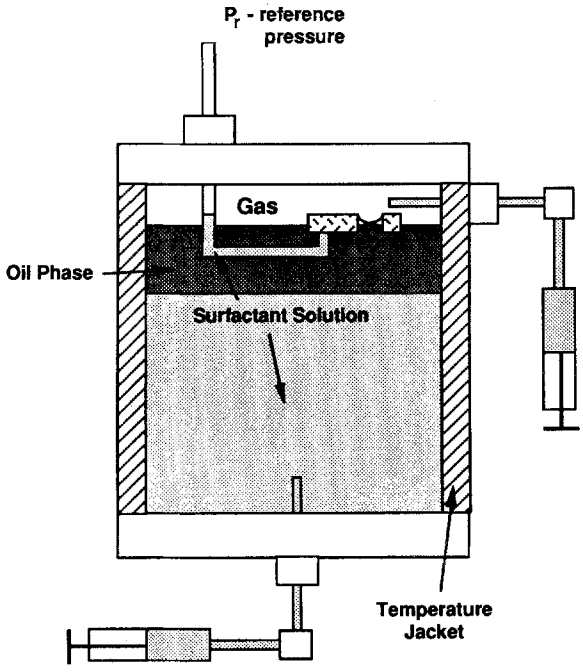

Fig. 1. Schematic of experimental cell.

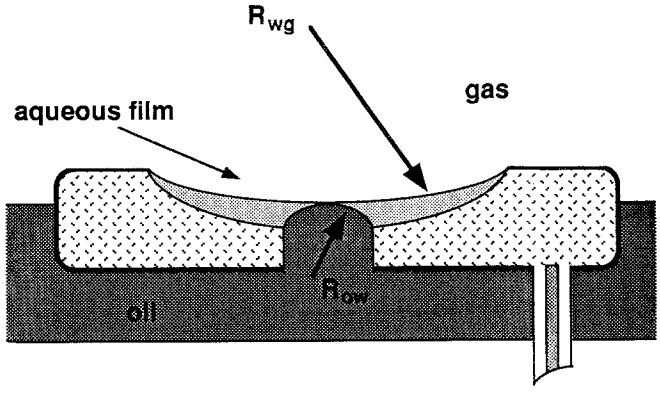

Fig. 2. Pseudoemulsion film porous-disk holder

film holder (see Fig. 1). Drops must be added carefully to prevent unwanted emulsification of the oil during film formation.

Accurate thickness and disjoining pressure measurements require plane-parallel thin-liquid films. For flat foam films in equilibrium, the disjoining pressure, Π, equals the capillary pressure, P_c, and can be measured directly:

$$P_c = P_g - P_w = \Pi(h)\,, \tag{1}$$

where P_g is the gas pressure, and P_w is the hydrostatic pressure in the Plateau border region. However, as illustrated in Fig. 2, to control capillary-induced curvature and produce plane-parallel pseudoemulsion films, the geometry of the hole used in the porous film holder is crucial. Flat films demand that the pressures on the gas and oil sides of the film be equal. This criterion leads to the following relation:

$$P_c = P_g - P_w = P_o - P_w = \frac{2\sigma_{wg}}{R_{wg}} = \frac{2\sigma_{ow}}{R_{ow}}\,, \tag{2}$$

where P_i is the pressure in phase i, and σ_{ij} is the tension between phases i and j, with the subscripts g, o, and w corresponding to gas, oil, and water (i.e., aqueous surfactant solution) phases, respectively. R_{wg} is the radius of curvature in the Plateau border region at the gas/water interface while R_{ow} is the radius of curvature at the oil/water interface. To satisfy Eq. (2) when the surface tension, σ_{wg}, differs from the interfacial tension, σ_{og}, we must carefully construct the film holders such that the curvature in the Plateau border region will compensate for the tension difference. That is, differences in R_{wg} and R_{ow} offset tension-induced bowing of the film.

How to accomplish this is pictured in Fig. 2. The porous frit is machined with diamond-studded drill bits to produce a frit geometry that generates relative curvature differences between the two Plateau border regions. This difference in curvature compensates for the tension difference and permits plane-parallel films in the center of the hole. Verification of a flat-film region is achieved by scanning the film-thickness over the entire region, to guarantee uniform readings. We also use visual observations from a video camera and in some cases employ Michelson interferometry (via an Ealing Electro-optics interference objective Model 25-0092) to measure the topography of the solution-air interface [13]. The exact hole geometry is determined by trial and error. Often different geometries are required to maintain plane-parallel films over a large range of capillary pressures. Generally, smaller hole diameters are required for higher pressures.

Films thickness

Film thicknesses are determined by the microinterferometric technique first developed by Scheludko [2, 14]. An indicent-light microscope, utilizing a heat-filtered 200 W Hg-Xe light source and equipped with two fiber optic probes (EG&G Gamma Scientific, Model 700-10-34A & – 37A), is used to monitor the intensity of reflected light from the film at a zero angle of incidence. The probes measure spot sizes of 14 and 45 μm and can be translated across the film to ensure a uniform film thickness. To

provide independent verification of the thickness, two different wavelengths (i.e. 546 and 665 nm) are monitored simultaneously with two highly sensitive photomultiplier tubes (RCA C3103402) mounted in thermoelectrically cooled housings (Products for Research Model TE-104). Additional details of the experimental apparatus can be found elsewhere [3,13].

By assuming a homogeneous film and neglecting absorption of light, we derive an expression to extract an optical thickness from the light reflected by film:

$$h_w = \left(\frac{\lambda}{4\pi n_w}\right)\arccos\left\{\frac{1}{2r_1r_2}\left(\frac{(1-r_1^2)(1-r_2^2)}{1-\Delta\left(\left(\frac{r_1+r_2}{1+r_1r_2}\right)^2-\left(\frac{r_1-r_2}{1-r_1r_2}\right)^2\right)-\left(\frac{r_1-r_2}{1-r_1r_2}\right)^2}\right)-(1+r_1^2r_2^2)\right\}, \quad (3)$$

where $\Delta = (I - I_{min})/(I - I_{max})$, $r_1 = (n_w - n_g)/(n_w + n_g)$, $r_2 = (n_o - n_w)/(n_o + n_w)$, n_i is the refractive index of phase i, h_w is the film thickness calculated assuming a homogeneous refractive index equal to the bulk solution value (i.e., $n_w = 1.33$), and λ is the wavelength of light. I is the value of the reflected intensity while I_{max} and I_{min} correspond to the interference maximum and minimum values. Equation (3) reduces to the standard optical model used for foam films by replacing Δ with $(1 - \Delta)$, to account for the difference in optical phase shifts, and by setting $r_1 = -r_2$ [13], Following Duyvis [15], an additional modification to the optical model is used to account for adsorbed surfactant at the film interfaces. However, since the refractive index of the surfactant tails closely matches that of the organic phase (dodecane) we apply the Duyvis optical correction for adsorbed surfactant layers to the air-film interface only. This two-layer treatment is consistent with the so-called three-layer model used for foam films; the corrected thickness is designated by h. The aqueous core thickness can be estimated from h_w by subtracting off ~ 1.2 nm from the adsorbed surfacant layer. Independent measurements of the film thickness with two different wavelengths agree to within ± 0.8 nm.

Materials

Three different surfactants are utilized in this study. Kodak electrophoresis grade (> 99%) sodium dodecyl sulfate, SDS, is used with no further purification. Surface tension versus concentration measurements on this surfactant reveal a shallow minimum around the CMC indicating trace amounts of impurities. Furthermore, SDS in aqueous solutions hydrolyzes to produce dedecanol as an impurity [16]. Therefore, solution age is carefully monitored so that meaningful comparison can be made. When equilibration with oil is required, solutions are aged for 3 days prior to use. We also use cetyltrimethylammonium bromide, CTAB, from Fluka and a commercial alpha olefin sulfonate that has a carbon chain length between 14 and 16, AOS 1416, supplied by Shell. No attempts were made to characterize their purity. Dodecane (> 99%) is obtained from Aldrich and is also used with no additional purification. All solutions are prepared with distilled water that is further purified with a four-stage Milli-Q reagent grade water system from Millipore.

Procedure

Equilibration between the oil and aqueous surfactant phase is accomplished by placing the less dense oil (dodecane) on the surface of the surfactant solution followed by gentle stirring from below with a magnetic stir bar. These conditions are maintained for at least 2 days before the phases are carefully separated and used for the disjoining pressure measurements. Once equilibrated, the separate phases are transferred to the measurement cell depicted in Fig. 1. To avoid stray reflections from the oil-aqueous solution interface during the experiment, the oil-layer thickness in Fig. 1 should exceed 2 cm.

After saturating the film holder with surfactant solution, a thick pseudoemulsion film is formed using the two syringe ports, as described earlier. To maintain vapor-liquid equilibrium throughout the experiment, surfactant solution is also placed in the gas phase and positioned close to the film. The gas pressure in the cell is then alternately increased and decreased slowly with a syringe to produce films that are locally plane-parallel, as observed visually, and that have thicknesses of the last interference maximum (I_{msx}) and minimum (I_{min}) needed in Eq. (3). As an added precaution, I_{min} and I_{max} values are carefully redetermined upon the conclusion of each experiment. After determining the interference extrema , the cell pressure is set to the desired value, and the capillary pressure exerted on the film is measured directly with differential pressure transducers (Omega Model PX750 – 06DI $\pm$ 0.5 Pa). In order to establish and measure accurate differential pressures below 100 Pa, the reference pressure, P_r in Fig. 1, must be isolated from

external fluctuations [13]. The reflected intensity of light from the film is monitored continuously and once equilibrium is established, the intensity and capillary pressure are recorded. For flat films in equilibrium, the capillary pressure equals the disjoining pressure. Therefore, we obtain the entire disjoining pressure isotherm by carefully increasing or decreasing the gas pressure in the cell.

Dynamic film thinning experiments are performed in an analogous manner. We subject a biconcave lens, formed in the film holder, to a step increase in the capillary pressure and hold it at a constant value. The evolution of film thickness versus time is then followed interferometrically, as outlined above. Additional experimental details can be found elsewhere [3, 13].

Results

Film thinning

A typical photocurrent versus time interferogram for a dodecane/air pseudoemulsion film exposed to a ~ 50-Pa capillary pressure is reproduced in Fig. 3. This particular film contains 1 wt% AOS 1416, which is well above the CMC. Also, 1 wt% glycerol is added to the aqueous phase to slow thinning and enhance the quality of the interferogram. We have verified that glycerol does not qualitatively affect stratification for this system. Since photocurrent is a direct measure of thickness, this curve represents the thinning behaviour for the film. The pronounced horizontal portions of the interferogram confirm that pseudoemulsion films undergo the same step-wise layer thinning previously observed in foam and emulsion films containing surfactant above the CMC [3, 17–31]. Although the interferogram shows only two distinct transitions, simultaneous video observations from a camera attached to the microscope confirm that two layers passed the optical probe after 2.5 min of thinning. Therefore, the transition from 51.9 nm to 26.3 nm actually corresponds to two transitions in quick succession. Thus, we find a total of three transitions for this system. It can also be noted that the photocurrent for a pseudoemulsion film rises as the film thins instead of declining as in symmetrical films (i.e, foam or emulsion). This simply arises from the differences in optical phase changes that take place upon reflection at the two interfaces. Consequently, pseudoemulsion films below 50 nm in thickness appear white while symmetrical films of comparable thickness appear black. An example of this is provided in Fig. 4. Here, we picture both a foam and pseudoemulsion film, photographed from the video monitor, as they undergo a thinning transition from 26 nm to 16 nm. This picture clearly shows the difference produced by the optical phase shifts while also revealing the striking similarities in the layer-transition process between foam and pseudoemulsion films. As detailed account of the transition dynamics, depicted in Fig. 4, has recently been given by Bergeron et al. [32].

Fig. 3. Typical pseudoemulsion film interferogram

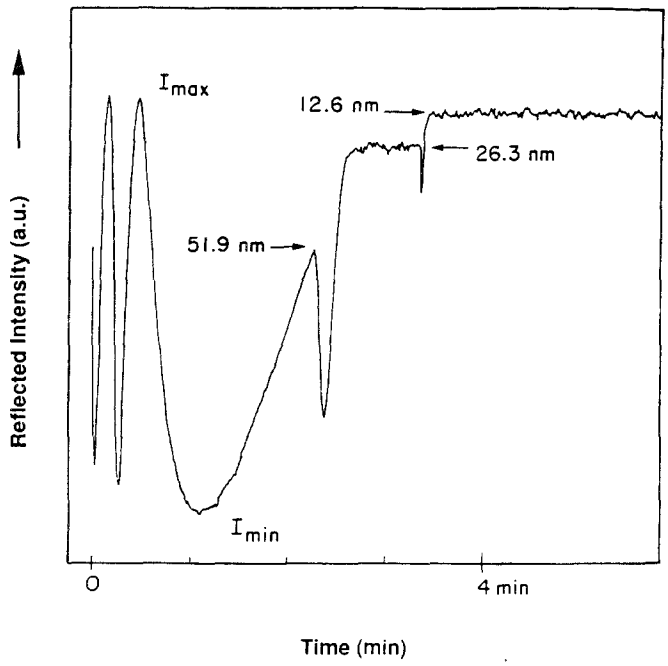

In addition to our observations on pseudoemulsion-film stratification, we also find that asymmetric gas/water/solid films can display multilayer thinning when stabilized with surfactant well above the CMC. By performing thinning experiments similar to those outlined above on aqueous CTAB films (0.2 M), sandwiched between air and glass, we observe behaviour extremely similar to that found for pesudoemulsion films. When these films are exposed to a ~ 50 Pa capillary pressure non-monotonic thinning (multiple white films) starts to occur at approximately 50 nm with as many as five layers being removed before an equilibrium thickness is established.

In Fig. 5, we directly compare the thinning behavior between stratifying (above the CMC) and nonstratifying (below CMC) foam films stabilized with aged (3 days) SDS. The dark circles in the figure correspond to a 0.1 M SDS solution, which is significantly above the CMC (0.008 M), while the open circles represent data for a 0.005 M SDS solution. Both films are kept at a constant film radius of 0.2 mm and a constant capillary pressure of 65 Pa. To achieve these conditions, different film holders, having holes bored with slightly different aspect ratios are required for each film. Lines are drawn in the figure to provide visual continuity of the data.

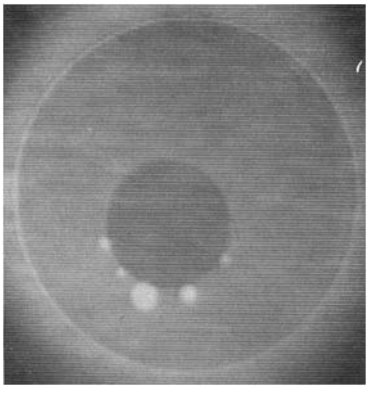

0.1 M SDS Foam Film

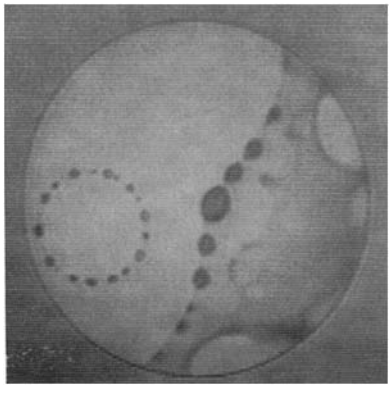

0.1 M SDS/Dodecane Pseudoemulsion film

Fig. 4. Photomicrograph of layer transition for thinning 0.1 M SDS (aged) foam and dodecane/air pseudoemulsion films

The 0.1 M data display three distinct transitions in film thickness starting at 60 nm. Each transition corresponds roughly to a 10 nm decrease in thickness which agrees well with literature values [24, 26, 27]. Eventually, the film reaches a metastable equilibrium thickness of 22 nm. Data for the 0.005 M SDS solution start around 50 nm, when the film becomes visually plane-parrallel, and exhibit smooth monotonic thinning behavior to an equilibrium thickness of 36 nm. If we define the film drainage time, t_d, by the time required to reach a (metastable) equilibrium thickness from 60 nm, we find that $t_d = 190$ s for the 0.1 M film and 260 s for the 0.005 M film.

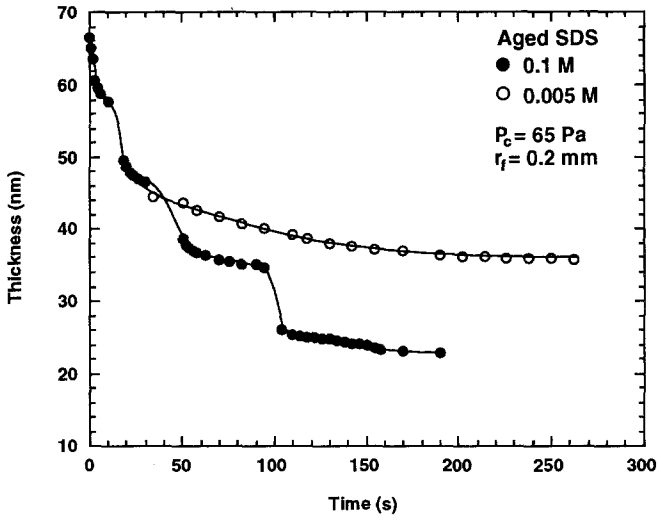

Fig. 5. Dynamic thinning curves for stratifying and non-stratifying SDS (aged) foam films

Disjoining pressure measurements

The disjoining pressure isotherms for both foam and pseudoemulsion films generated from 0.1 M, fresh (several hours) SDS solutions are displayed in Fig. 6. This concentration of SDS is well above the CMC, but only produces spherical micelles in the bulk aqueous solution. The open circles represent data for a foam film made from a fresh SDS solution, while filled circles correspond to a dodecane/air pesudoemulsion film. Both isotherms reveal four distinct branches, the thickest at 50 nm followed by subsequent branches that repeat at regular intervals of approximately 10 nm as film thickness decreases. We also find that the transition pressure (i.e, the maximum pressure reached before the transition to the next stable branch) increases as the film becomes thinner. Gaps in the data between branches identify thermodynamically unstable regions of the isotherm where the slope, $\partial\Pi/\partial h$, is positive [33]. The arrow in Fig. 6 indicates that the final branches at approximately 16 nm continue to even higher disjoining-pressure values. This high-pressure extension of the isotherms is presented in Fig. 7.

The pressure scale in Fig. 7 is changed to kPa, and the ordinate is plotted on a logarithmic scale, otherwise the symbols and the experimental conditions used in Fig. 7, are identical to those in Fig. 6. Data for the pseudoemulsion film terminate around 0.2 kPa, corresponding to rupture of the film. The foam film, however, remains stable beyond 10 kPa and its rupture pressure exceeds the highest pressure experimentally accessible with our apparatus.

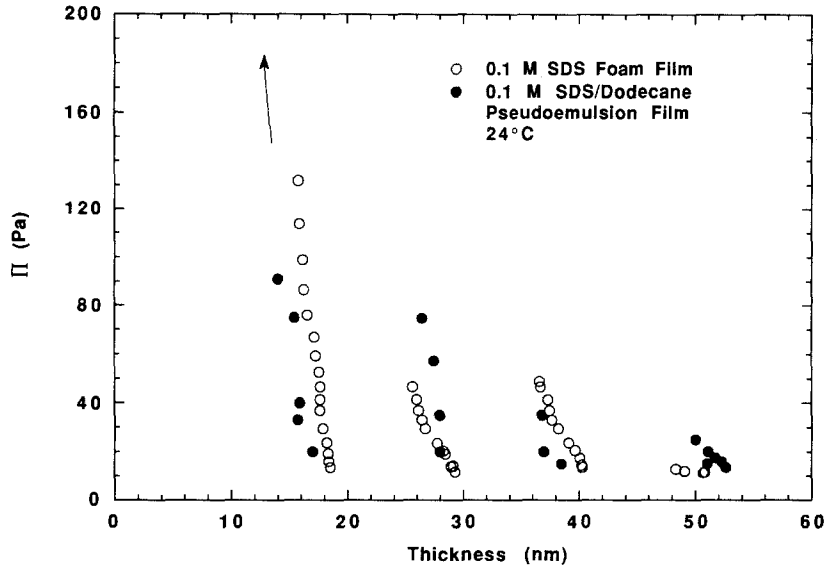

Fig. 6. Low-pressure region of the disjoining pressure isotherm for 0.1 M SDS (fresh) foam and dodecane/air pseudoemulsion films

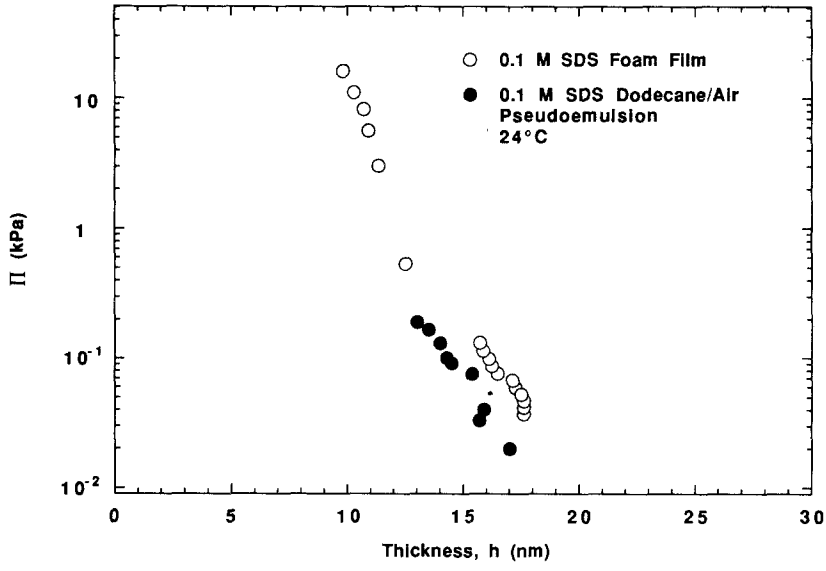

Fig. 7. High-pressure region of the disjoining pressure isotherm for 0.1 M SDS (fresh) foam and dodecane/air pseudoemulsion films

At the higher pressures, a Newton black film approximately 4.5 nm thick does exist for this foam system, but we have not characterized it quantitatively.

Discussion

The comparison in Fig. 5 reflects how thinning behavior is influenced by the form of the disjoining pressure isotherm. The connection becomes apparent when we consider the driving force for film thinning, P_c-$\Pi(h)$. The $\Pi(h)$ isotherm for the 0.1 M SDS solution is oscillatory with a series of unstable ($\partial\Pi/\partial h > 0$) regions approximately spaced at 10 nm intervals (See Fig. 6). The onset of these regions corresponds precisely to the sharp transitions (i.e., stratification) observed in Fig. 5. Transitions shown by the interferogram and the micrographs in Figs. 3 and 4, respectively, arise from the same conditions. Conversely, the 0.005 M solution used in Fig. 5 has a monotonically increasing disjoining pressure and the film thins uniformly to its equilibrium thickness.

Although the 0.005 M SDS films rupture at lower capillary pressures (i.e, are less stable) than 0.1 M films, they actually thin more slowly to thicker equilibrium films under the present conditions. Again, this behavior reflects the form of the disjoining pressure isotherm. 0.1 M films

have a higher ionic strength which lowers the Debye length and the distance for interaction between the interfaces. This allows the 0.1 M films to thin faster. In this case, force barriers, generated by surfactant structuring, are too low to affect significantly the driving force, P_c-Π(h). The oscillatory component to the disjoining pressure curve is small and has little effect on thinning dynamics except at very low P_c. Furthermore, structuring in the 0.1 M SDS films does not appear to increase the viscosity of the fluid in the film. Our dynamic thinning measurements for 0.2 M CTAB gas/aqueous/solid films also confirm this result which is further supported by recent theoretical findings [34].

Increases in the ionic strength for the higher surfactant concentration lead to a higher adsorption of surfactant at the interface and provide the 0.1 M films with stronger short-range repulsive forces that stabilize the film. This explains the increased stability over the 0.005 M films. Film stability is inevitably derived from the repulsive forces that generate the common and Newton films. Dynamic interfacial properties may also contribute to the kinetic stability of a film [35, 36], but in the present case time scales for thinning are sufficiently long to establish an equilibrium configuration [3].

Figure 6 clearly demonstrates that the oscillatory component of the disjoining pressure isotherms, for the foam and pseudoemulsion films studied, is practically identical. In both cases, the negatively sloping region of each oscillation in the isotherm is carefully scanned by increasing and decreasing the capillary pressure while remaining on one individual branch. This confirms that films existing in these regions are indeed in a metastable equilibrium state.

Previously, stratifying behavior in foam films has been attributed to either repeating units of surfactant bilayers [24, 26] or to a cubic lattice of ordered micelles [27]. These same concepts can be applied to explain the origin of the oscillatory component measured in Fig. 6. In fact, Laso [34] has recently used density functional theory (DFT) to calculate oscillatory disjoining pressures from aqueous micellar solutions. These calculations support the supposition that micelles order within the film.

Although no direct evidence exists for micellar structuring, Wasan et al. [31] have shown that films containing latex spheres produce stepwise thinning behavior similar to that observed in micellar films. However, neutron reflection experiments at the air-water interface of an SDS solution above the CMC also suggest structures that may have bilayer-like character [37]. Further evidence for bilayer structuring is also found by Exerowa and Lalchev [38], who measure step wise transitions in the disjoining pressure isotherm for multicomponent foam films which contain phospholipids. It seems likely that both types of structuring (micellar and bilayer) are possible and may not be mutually exclusive [3]. The particular form of self-assemblage depends strongly on the type and concentration of surfactant present as well as other system parameters that commonly affect bulk phase behavior.

Disjoining pressure data in Fig. 6 involves both systems equilibrated with oil (pseudoemulsion films) and those that are oil free (foam films). The excellent agreement shown in Fig. 6 between foam and pseudoemulsion film data indicates that oil solubilization does not significantly affect film stratification under the conditions we have tested. In fact, the presence of oil seems to reduce SDS aging effects [3]. We expected the pseudomulsion films to compare more closely to aged SDS foam films, because phase equilibration allows the surfactant solution to age and produce dodecanol via SDS hydrolysis. Instead, more favorable agreement is found with foam films made from fresh solutions, as seen in Fig. 6. Apparently, during equilibration the oil (dedecane) scavenges dodecanol produced by SDS degradation, thereby lowering alcohol contaimination of the interfaces.

Once the films in Fig. 6 thin below 20 nm no further evidence for surfactant microstructures remains and continued increases in pressure eventually lead to rupture of the film. Figure 7 reveals that the pressure required to rupture SDS pseudoemulsion films is lower than that for SDS foam films by at least two orders of magnitude. Further, in both cases film-rupture pressures ($\sim$ kPa) are significantly higher than the branch-transition pressures ($\sim$ Pa) measured in Fig. 6. This suggests both that SDS pseudoemulsion films are less stable (i.e, they rupture at a lower P_c) than their foam counterparts, and that overall film stability is not significantly influenced by film stratification.

The lower stability of pseudoemulsion films demonstrated in Fig. 7 cannot be explained by simple application of DLVO theory. Surface tension versus SDS concentration data indicate that adsorption of surfactant at the air-water and oil-water interface is essentially the same ($\sim 3.5 \times 10^{-10}$ mol/cm^2) [39]. Consequently, we expect the surface charge density to be similar at both interfaces. This in turn should produce the same repulsive electrostatic component to the disjoining pressure isotherm. Within the framework of DLVO theory we must also add a contribution to the disjoining pressure from London–van der Waals dispersion forces. For the dodecane/water/air system, we find that this contribution helps to stabilize the pseudoemulsion film (i.e., negative Hamaker constant) while the foam films are destabilized (i.e, positive Hamaker constant) [40]. Therefore, simple application of DLVO theory predicts that our pseudoemulsion films are more stable than foam films. This is quite the opposite of

experimental observations. The same conclusion is also reached if we incorporate an adsorbed surfactant/oil layer at the interface into the DLVO model [41].

A possible explanation for decreased pseudoemulsion film stability is that the so-called hydrophobic force may be operative in these films. Recently, it has been shown that hydrophobic interfaces display attractive forces much greater than those predicted by DLVO theory [42]. Although anionic surfactant is adsorbed at the oil-water interface in our pseudoemulsion films, the presence of dodecane does suggest a much higher hydrophobic environment than in foam films. This may lead to attractive forces similar to those observed at other hydrophobic interfaces. Unfortunately, no definitive explanation for the hydrophobic interaction exists.

Summary

Asymmetric films formed from aqueous surfactant solutions above the CMC undergo film stratification analogous to that observed in foam and emulsion films. Thinning experiments on dodecane/air pseudoemulsion films made from anionic surfactant solutions of 1 wt% AOS 1416 display three discrete thickness transitions. Similarly, aqueous 0.2 M CTAB films sandwiched between glass and air produce as many as five transitions. Although white instead of black (due to optical phase changes upon reflection at the interfaces), these multilayered films arise from the same supramolecular ordering produced in symmetric micellar films.

We also measure the disjoining pressure isotherms for dodecane/air pesudoemulsion films stabilized with 0.1 M SDS, which is well above the CMC. These measurements reveal, for the first time, an equilibrium oscillatory component to the isotherm that extends to film thickness greater than 50 nm and has a periodicity on the order of 10 nm. The oscillatory forces originate from surfactant structuring within the film and are responsible for the stepwise thinning these films display. As film thickness decreases, the slope and peak height of each subsequent branch in the isotherm increases.

Comparison is made between disjoining pressure isotherms for foam and pseudoemulsion films generated from 0.1 M SDS solutions. At low capillary pressures, the oscillatory component produced in both films is practically identical. The magnitude of the branch-transition pressures, and the location of transitions in film thickness are essentially the same. However, the high-pressure region of the isotherms indicates that pseudoemulsion films rupture at significantly lower capillary pressures (0.2 kPa) than their foam counterparts (> 10 kPa). This observation is consistent with the finding that foam is destabilized by oil, as found previously in bulk foam and porous-media tests [5–9]. Our data indicate that film stability results from the repulsive common and Newton film branches of the isotherm and that stratification only influences film thinning when the imposed capillary pressure is very low. Otherwise, forces generated by surfactant structuring in 0.1 M SDS films are too small to affect significantly the stability of the film. Other stratifying systems seem to produce more significant forces [38, 43] which may result from different types of macrostructuring in the film.

Acknowledgement This work was supported by the Assistant Secretary for Fossil Energy, Office of Oil, Gas, and Shale Technologies of the U.S. Department of Energy under Contract DE-AC03-76SF00098 to the Lawrence Berkeley Laboratory of the University of California.

References

1. Derjaguin BV, Churaev NV, Muller VM (1987) In: Kitchener JA (ed.) Surface forces. Consultants Bureau New York
2. Scheludko A (1967) Advan Colloid Interface Sci 1:391–464
3. Bergeron V, Radke CJ (1992) Langmuir 8:3020–3026
4. Richetti P, Kékicheff P (1992) Phys. Rev Let 68 No. 12, 1951–1954
5. Wasan DT, Nikolov AD, Huang DD, Edwards DA (1988) In: Smith ed. Surfactant Based Mobility Control – Progress in Miscible–Flood Enhanced Oil,Recovery ACS Symp. Series 373 American Chemical Society Washington D.C. Chapter 7: 136–162
6. Manlowe DJ, Radke CJ (1990) Soc. Petroleum Eng. Reservior Eng 5 No. 4, 495–502
7. Bergeron V, Fagan ME, Radke CJ, (1993) Langmuir 9, No. 7, 1704–1713
8. Kurglyakov PA (1988) In: I.B. Ivanov, ed., Thin Liquid Films – Fundamentals and Applications, Marcell Dekker Inc., New York, Chapter 11, 767–827
9. Koczo K, Lobo LA, Wasan DT, (1992) J Colloid Int Sci 150 No. 2, 492–506
10. Bergeron, V Radke CJ (1991) In: Proceedings of the 6th Research Conference on Exploration – Production, Physical Chemistry of Colloids and Interfaces in Oil Production, Saint-Raphaël France, Editions Techinip, Paris.
11. Mysels KJ, and Jones MN (1966) Discuss Faraday Soc 42: 42–50
12. Exerowa D, Kolarov T, Kristov KHR (1987) Colloids and Surf 22: 171–185 (1987)
13. Bergeron V (1993) Ph D Thesis, University of Calofornia Berkeley California
14. Scheludko A (1957) Kolloid Zeit 155:39–44
15. Duyvis EM (1962) Thesis, Utrecht
16. Muramatsu M, Inoue M (1976) J Colloid Interface Soc 55:80–84
17. Johonnott ES (1906) Phil Mag, 11:746–753

18. Perrin J (1918) Ann Phys 10:160–184
19. Rickenbacher W (1916) Kolloid Chem Beihefte 8:139–170
20. Wells PV (1921) Ann Phys 16:69–110
21. Dewar J, (1927) in: L. Dewar, ed. Collected Papers of Sir James Dewar Vol. II Cambridge, 1170–1172
22. Bruil HG, Lyklema J (1971) J. Nature Phys Sci 233:19–20
23. Friberg S, Linden E, Saito H (1974) Nature 251:494–495
24. Keuskamp JW, Lyklema J (1975) In: Mittal KL ed. Adsoprtion at Interfaces ACS Symposium Series 8 Washington DC 191–198
25. Manev E, Proust JE, Ter-Minassian-Saraga, (1977) Colloid and Polymer Sci 255:1133–1135
26. Manev ED, Sazdanova SV, Rao AA, Wasan DT (1982) J Dispersion Sci and Technol 3:435–463
27. Nikolov AD, Wasan DT (1989) J Colloid Interface Sci 133:1–12
28. Nikolov AD, Wasan DT, Denkov ND, Kralchevsky PA, Ivanov IB (1990) Progr Colloid Polym Sci 82:87–98
29. Manev ED, Sazdanova SV, Wasan DT (1984) 5:111–117
30. Bergeron V, Radke CJ (1991) In: Toulhoat H, Lecourtier J (eds) Proceedings of the 6th Research Conference on Exploration-Production, Physical Chemistry of Colloids and Interfaces in Oil Production, Editions Techinip Pairs Vol 1.
31. Wasan DT, Nikolov AD, Kralchevsky PA, Ivanov IB (1992) Colloids and Surfaces, 67:139–145
32. Bergeron V, Jiménez-Laguna AI, Radke CJ (1993) Langmuir, 8:3027–3032
33. Scheludko A (1962) Proc Koninkl Ned Akad Wet B65:87–96
34. Laso M (1993) Ph D Thesis University of California Berkeley CA
35. Scriven LE, Sternling CV (1960) Nature 187:186–188
36. Malhotra AK, Wasan DT (1988) In: Ivanov IB, (ed.), Thin Liquid Films-Fundamentals and Applications, Marcel Dekker: New York, Vol 29, 829–890
37. Lee EM, Simister EA, Thomas RK, Penfold J (1989) Colloque de Physique, 50:75–81
38. Exerowa D, Lalchev Z (1986) Langmuir, 2:668–671
39. Rehfeld S (1967) J Phys Chem, 71:38–745
40. Israelachvili JN (1985) In: Intermolecular and Surface Force – with Application of Colloidal and Biological Systems, Academic Press Inc, Orlando Fl: 137–159
41. Hirasaki GJ (1991) Soc. Petroleum Engr Formation Evaluation 6 No. 2: 217–226
42. Israelachvili JN, Pashley RM (1984) J Colloid Int Sci. 98, No. 2, 500–514
43. Khristov Kh I, Ekserova DR, Kruglyakov PM, Fokins NT (1992) Kolloidnyi Zhurnal 54 No. 1: 173–178